

Confrontation with the Experience of 48 Combinations of Models of the Thermal and Electrical Behavior of Crystalline Solar Modules

M. Zouine[‡], A. Bennouna, N. Aarich, M. Akhsassi, N. Erraissi, M. Raoufi

Physics department - Faculty of Sciences Semlalia Marrakech - My Abdellah Avenue- Cadi Ayyad University Morocco

(meryem.zouine.ma@gmail.com, sindibad@uca.ma, aarich.noura@gmail.com, ingeniemohamed@gmail.com, erraissi.nouredine@gmail.com, raoufi@uca.ma)

[‡]Corresponding Author; Meryem Zouine, Cadi Ayyad University- Faculty of Sciences Semlalia Marrakech,

Tel: +212 672 607 419, meryem.zouine.ma@gmail.com

Received: 14.02.2021 Accepted: 11.03.2021

Abstract- Photovoltaic (PV) performance predictions are important to accurately assess the efficiency of any PV technology. In this study, we confront outdoor data with no less than 48 couples obtained by combining eight models of the thermal behavior with six electrical formulas. Calculations are confronted to the power produced by a 2 kWp grid-connected monocrystalline Si photovoltaic plant (GCPV) installed on the rooftop in the Faculty of Science Semlalia Marrakech, Morocco (latitude 31.6497 °N, longitude 8.0169 °W). The measured meteorological parameters (irradiance and air temperature), electrical data (DC power), and modules temperature data from one year have been used. The approach to evaluate the quality of each couple of models is new since this work uses the combination of (i) the best mix of correlation coefficient (R^2) and root mean square error (RMSE), and (ii) the number of points validated by the model within a 99% confidence interval. Among the eight thermal behavior models, we propose ourselves a dynamic one which takes into consideration inertia which is usually ignored in stationary models.

Keywords Grid-connected PV, PV DC-power measurements, Module temperature measurements, PV DC-power models, Module temperature models, Combinations of DC-power and module temperature models.

1. Introduction

The number of photovoltaic systems plants has been significantly increased over the last decade, for this purpose, extensive studies on the performance of installations PV plants have been carried out by various researchers [1]–[7]. Thus, with the dissemination of photovoltaic applications, the interest in correctly predicting the production of grid-connected photovoltaic (GCPV) systems has increased. But before even doing actual forecast, which itself introduces its own underlying errors induced by meteorological prevision, it is essential to have the best models to predict the performance of GCPV systems. There are several formulas giving the electrical power generated by modules [8] according to the solar irradiation and the cell temperature but the physical behavior of this last is itself described by several models depending themselves on solar irradiation, ambient temperature, and wind (as a minor contribution) [9].

There are many models expressing PV array power as a function of temperature such as Hendrie [10], Kroposki [11], King [12], Patel [13], Jie [14] and many others [15], [16]. A lot of other correlations can be found in the literature. Considering the importance of PV cell temperature in PV power analysis, this paper used thermal models for PV systems as a function of weather data (the ambient temperature, solar radiation, and wind speed), such as, Faiman et al [17], Mattei et al [18] and Sandia [19].

For each of the 48 couples of models, the PV module temperature and array output power are calculated from the five minutes-step meteorological parameters set (solar radiation, ambient temperature, and wind speed) and compared with the related 5 minutes-step field measured data. For this work, we used data from a PV power plant located in the Faculty of Sciences Semlalia Marrakech, Morocco. This PV field includes three silicon PV technologies and is equipped with an acquisition system for solar radiation, ambient, and cell temperature as well as wind speed [20]. In this paper, we chose to focus on monocrystalline silicon modules simply because the

technology is the oldest and the models are a little more consensual than for thin films or other recent technologies.

The paper is organized as follows: Section 2 deals with the description of the grid-connected photovoltaic system (GCPVS) and its database. Section 3 presents the PV cell temperature models while Section 4 is devoted to those predicting the DC power of the GCPV plant. The results are presented and discussed in Section 5.

2. Description of a grid-connected photovoltaic system (GCPVS) and its database

Fig. 1 shows the GCPV system that is installed at the Faculty of Science Semlalia Marrakech (latitude 31.6497 °N and longitude 8.0169 °W) in Marrakech. The PV modules shown in the front of the photograph are composed of monocrystalline silicon cells totaling a nominal power of 2040 W. The field is composed of a single string of 8 modules in series, with 255 Wp peak power for each Solar World AG “Sun-module Plus” (SW-255-mono).

The PV power of monocrystalline silicon technology was evaluated for one entire year, from May 2016 to April 2017. The 8 photovoltaic modules composing this system are south oriented and 30 tilt angled. A Sunny Boy SB 2000 inverter converts DC to AC with a maximum AC power of 2100 W. The nominal specifications of the modules are listed in Table 1.



Fig. 1. The GCPV system installed at the Faculty of Science Semlalia Marrakech

Table 1. Nominal specifications of the photovoltaic plant

Technology	Monocrystalline Si
Number of strings per plant	1
Number of modules per string	8
Nominal / Actual total power (Wp)	2040 / 2077
Nominal open-circuit voltage (V)	302.4
Nominal voltage at maximum power (V)	251.2
Nominal short circuit current (A)	8.66
Nominal current at maximum power (A)	8,15
Modules orientation (°)	0 (facing South)
Modules tilt angle (°)	30

The left photograph of Fig. 2 shows the weather station installed to measure and record the meteorological

parameters : radiation intensity E , ambient temperature T_a , wind speed V , and its direction. While, the right photograph of the same figure shows the box collecting the electrical data from both DC and AC sides of the inverter (voltages V , currents I , and powers P) as well as the cell temperature T_c , based on EEC standards the errors of measuring devices are considered in [21].



Fig. 2. Weather station (left) and electrical data acquisition system nearby the inverter (right).

3. Selected PV cell temperature models

According to the work done by Skoplaki and Palyvos [8], the PV cell temperature module varies depending on solar irradiance, wind speed, ambient temperature and material properties of the modules.

Many papers have used PV cell temperature models, for this reason we will refer only to those which are themselves devoted to the development of a model. With data collected from the GCPVS, we calculated the module operating temperature using solar irradiance (G_g), ambient temperature (T_a) and wind speed (V_w). But beyond what was done in a previous work [22], we will use these here to estimate the PV DC power. The list of models is not exhaustive.

Here, we focus on eight models, four models are presented by Lasnier [23], Akhsassi 1[24], Sandia [19] and NOCT [9]. Without taking in to account the wind speed. While, the four other models presented by Mattie [18], Faiman [17], Akhsassi 2 [22] and PVSyst [25] are influenced strongly by the wind speed. These models include also, as parameters, optical properties of the modules' components such as solar absorptance of PV layer (α), transmittance of glazing (τ), etc.

A selected group of PV temperature models to be used is presented in Table 2.

Table 2. Selected PV module temperature models

Groups	Correlations	Comments	Ref.
Without Wind speed	$T_c = T_a + \frac{G_g}{800} (T_{NOCT} - 20)$ (1)	NOCT , $T_{NOCT} = 46^\circ\text{C}$	[9] [26]
	$T_c = 30 + 0.0175(G_g - 300) + 1.14(T_a - 25)$ (2)	Lasnier ,	[23]
	$T_m = T_{ref} + C_1(G_g - G_{200}) + C_2(T_a - T_{a,NOCT})$ (3)	Akhsassi 1 , $T_{ref} = 25^\circ\text{C}$, $C_1 = 0.0123\text{K/W/m}^2$ $C_2 = 1.0396$, $T_{a,NOCT} = 20^\circ\text{C}$	[24]
	$T_m = T_a + G_g e^{(a+bv)}$ (4)	Sandia , $a = -3.56$, $b = -0.075 \text{ s/m}$	[19] [27]
Using Wind speed	$T_c = T_a + \frac{[1 - \eta_{PV\text{Syst}}](\tau\alpha)G_g}{U_{L0} + U_{L1}v}$ (5)	PVSyst , $\eta_{PV\text{Syst}} = 0.1$, $U_{L0} = 29\text{W/m}^2/^\circ\text{C}$ $U_{L1} = 0\text{W.s/m}^3/^\circ\text{C}$	[25] [28]
	$T_m = \frac{U_L T_a + \left[(\tau\alpha) - \eta_{STC} (1 - \beta_{STC} T_{ref}) \left(1 + \gamma_{Pmp} \ln \left(\frac{G_g}{G_0} \right) \right) \right] G_g}{U_L + \eta_{STC} \beta_{STC} \left(1 + \gamma_{Pmp} \ln \left(\frac{G_g}{G_0} \right) \right) G_g}$ (6)	Akhsassi 2 , $\gamma_{Pmp} = 0.04$ $U_L = 24.68 + 6.13 v$ $\eta_{STC} = 0.15$ $\beta_{STC} = 0.0045$	[22]
	$T_c = \frac{U_L T_a + [(\tau\alpha) - \eta_{STC} (1 - \beta_{STC} T_{ref})] G_g}{U_L + \eta_{STC} \beta_{STC} G_g}$ (7)	Mattei , $U_L = 26.6 + 2.3 v$ Others, same as used for Akhsassi2	[18]
	$T_m = T_a + \frac{s}{U_{L0} + U_{L1}v}$ (8)	Faiman , $S = (\tau\alpha)G_g$, $U_{L0} = 30.02\text{W/m}^2/^\circ\text{C}$ $U_{L1} = 6.28\text{W.s/m}^3/^\circ\text{C}$	[17] [29]

Back-surface module and cell temperatures become significantly different for high solar radiation intensities. The Sandia cell temperature model estimates cell temperature from module temperature T_m , plane of array irradiance G_g , and a temperature difference parameter ΔT_0 . They can be related by a simple relationship given in the equation bellow, this temperature difference was evaluated by King et al. [12] to be about $\Delta T_0 = 3^\circ\text{C}$ at an irradiance level of $G_0 = 1000\text{W/m}^2$. The module temperature is then given by:

$$T_m = T_c - \frac{G_g}{G_0} \Delta T_0 \quad (9)$$

Table 3. Selected PV DC power models

Correlations	Comments	Ref.
$P = \eta_{T_{ref}} A G_T (\tau\alpha) [1 - \beta_{ref} (T_c - T_{ref})]$ (10)	Hendrie (1979) , $T_{ref} = 25^\circ\text{C}$, $\eta_{T_{ref}} = 0.15$, $\tau\alpha = 0.81$, $\beta_{ref} = 0.0045^\circ\text{C}^{-1}$	[10]
$P = \eta_{T_{ref}} A G_T [1 - \beta_{ref} (T_c - T_{ref})]$ (11)	Jie (2007) , $\eta_{T_{ref}} = 0.14$	[14]
$P = \eta_{T_{ref}} A G_T [1 - \beta_{ref} (T_c - T_{ref}) + \gamma \log_{10} G_T]$ (12)	Cristofari (2006) , $\beta_{ref} = 0.0045^\circ\text{C}^{-1}$, $\gamma = 0.12$	[15]

4. Selected PV DC power models and implementation method

The PV cell temperature described in Section 3 is employed for predicting the DC power produced by the 2 kW_p grid-connected PV plant. Six models are proposed for this work to predict the PV DC power (see Table 3). The input parameters are the cell temperature and the solar irradiance, while the output is the power produced by the PV plant. The list of models is not exhaustive.

$P = P_{\max,ref} \frac{G_T}{G_{T,ref}} [1 + \alpha(T_c - T_{ref})][1 + \beta_{ref}(T_c - T_{ref})][1 + \delta(T) \ln \left(\frac{G_T}{G_{T,ref}} \right)] \quad (13)$	Kroposki (2000) , Coefficient δ evaluated at actual conditions	[11]
$P = P_0 \frac{G_T}{G_{ref}} [1 + (\alpha - \beta_{ref})\Delta T] \quad (14)$	Patel (1999) , $\alpha = 0.0005 \text{ } ^\circ\text{C}^{-1}$, $\beta = 0.005 \text{ } ^\circ\text{C}^{-1}$	[13]
$P = P_{\max,ref} [1 - D_f(T_c - 25)] \quad (15)$	Al-Sabounchi (1998) , $D_f = \text{deficiency factor} = 0.005 \text{ } ^\circ\text{C}^{-1}$	[16]

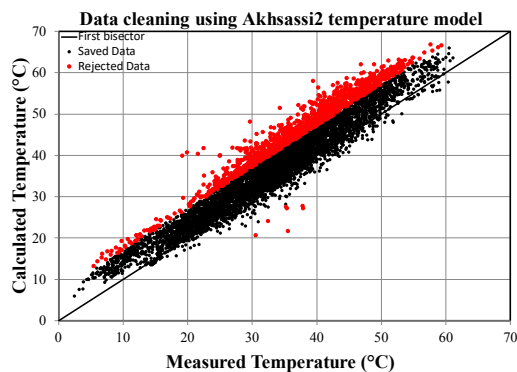
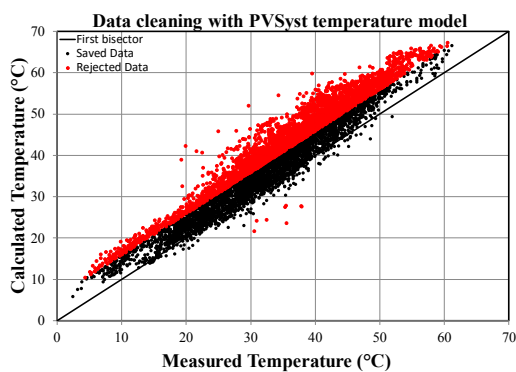
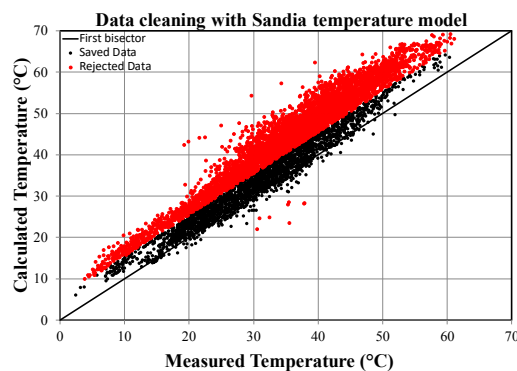
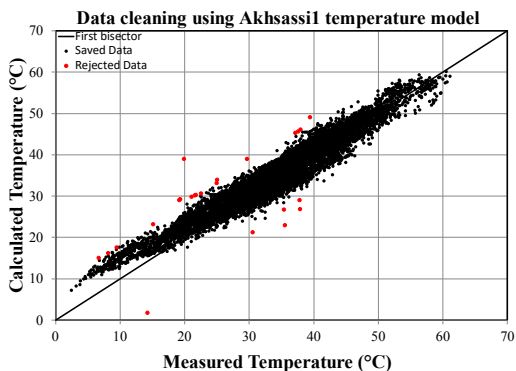
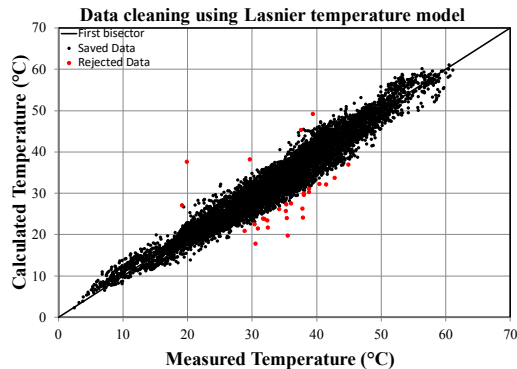
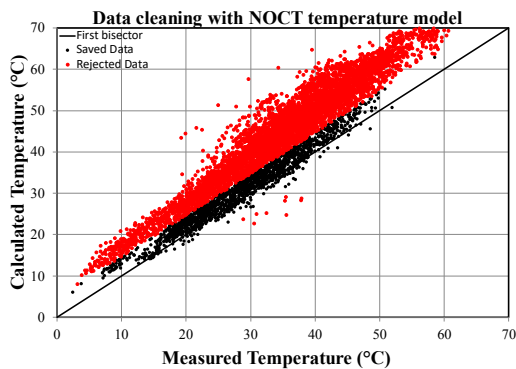
5. Results and discussion

5.1. Stationary regime

For one year, 6714 sets of data were recorded from which we will first focus on identifying and removing inappropriate records (inaccurate "normal" or mistaken records). For a normal distribution of measured values around mean, there are less than 1% of inaccurate data lying outside the band around the mean [mean - 3×RMSE, mean + 3×RMSE]. Considering that working with 99% of acceptable "normal" data is sufficient, all the data sets outside this interval are removed, which, in addition to the 1% of "normal" inaccurate data, also removes other types of abnormally mismatching data. The new RMSE is

calculated and the removal step is repeated until no data is outside the interval [22].

Figure 3 shows the effect of our cleaning which has removed a cloud of several points above the average. Apart from spurious points which might be in the peripheral area, this cloud of points can be considered as overestimation of the PV temperature using the models of, NOCT and Sandia among the models with no wind velocity, also for all the fourth models using wind velocity in their equations. Fig. 3 shows one of the visual aspects of the cleaning of the eight thermal models, where 31 points are removed using the Lasnier model while 5462 points are removed using the Mattei model.



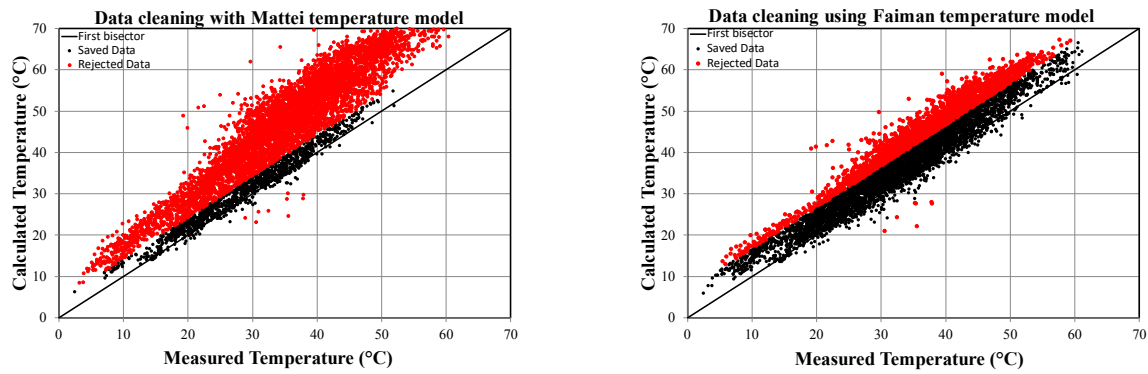


Fig. 3. Predicted versus measured PV cell temperature for 6714 experimental data. The red circles are the eliminated data after the cleaning while the black circles are kept. The continuous line represents the first bisector.

It is noticed that the models considering wind velocity variation had been the least accurate compared to the models not taking the wind velocity effect into account which we had expected since the wind speed has never exceeded 19.20 km/h during the entire year, hence it reached the peak only once during the 6714 recorded times and it was on the 30/8/2016 at 18h25 with 5.336m/s only, which does not contradict with climatic conditions as known in the area of Marrakech since it is considered internationally as a non-windy zone.

On the 1st of January 2017, 1 hour after the sunrise, we have recorded a $T_a=9.149^{\circ}\text{C}$, $G=334,442\text{W/m}^2$ and $W_v=0,400\text{m/s}$ while the measured Temperature was $11,53^{\circ}\text{C}$; the predicted temperature for each thermal model is:

- NOCT Temperature: $19,02^{\circ}\text{C}$.
- Lasnier Temperature: $11,53^{\circ}\text{C}$.
- Akhsassi1 Temperature: $15,38^{\circ}\text{C}$.
- Sandia Temperature: $18,38^{\circ}\text{C}$.
- PVSyst Temperature: $17,49^{\circ}\text{C}$.
- Akhsassi2 Temperature: $16,88^{\circ}\text{C}$.
- Mattei Temperature: $20,22^{\circ}\text{C}$.
- Faiman Temperature: $17,48^{\circ}\text{C}$.

The 6th Mai 2017, when the sun passes to the zenith, we have recorded $T_a=28,329^{\circ}\text{C}$ $G_g=955,619\text{W/m}^2$ $W_v=0.133\text{m/s}$, while the measured Temperature was $44,633^{\circ}\text{C}$; the predicted temperature for each thermal model is:

- NOCT Temperature: $56,52^{\circ}\text{C}$.
- Lasnier Temperature: $42,40^{\circ}\text{C}$.
- Akhsassi1 Temperature: $42,99^{\circ}\text{C}$.
- Sandia Temperature: $55,24^{\circ}\text{C}$.
- PVSyst Temperature: $52,15^{\circ}\text{C}$.
- Akhsassi2 Temperature: $52,64^{\circ}\text{C}$.
- Mattei Temperature: $61,81^{\circ}\text{C}$.
- Faiman Temperature: $53,42^{\circ}\text{C}$.

The experience shows that most of the thermal models had overestimated the PV module temperature, this phenomenon can be explained by the dynamic effects when increasing abruptly the incident solar radiation intensity with thermal inertia involved, the PV temperature makes a delay to gain this new excited temperature and vice versa, the dynamic effect is studied in section5.2.

Table 4 shows the statistical results of the correlation coefficients R^2 and RMSE before and after each cleaning. Lasnier and Akhsassi1 models removed less than 0.5% of the dataset and nevertheless, their R^2 were improved by 20%. NOCT, PVsyst, Mattei, and Sandia models removed more than 45% from the dataset essentially caused by an overestimation of the temperatures. In the other hand the best R^2 and RMSE values belongs to Mattei model with 98.67% and 1.43°C , still it cannot be taken as the best thermal model since 81.35% of the total points were removed after cleaning. In the meantime, Lasnier R^2 has reached 97.16% with an RMSE of 2.53°C and with the minimum data removal.

Table 4. Descriptive statistics of original and processed data sets for the eight PV cell temperature models

	Statistical correlations						Cleansing statistics		
	R^2		RMSE ($^{\circ}\text{C}$)		NRMSE		% removed REM	Saved Data	Deleted Data
	Before	After	Before	After	Before	After			
NOCT	82,77%	98,48%	6,00	1,58	0,102	0,028	75,60%	1638	5076
Lasnier	77,44%	97,16%	6,76	2,53	0,115	0,043	0,46%	6683	31
Akhsassi 1	76,85%	96,87%	6,84	2,65	0,117	0,050	0,39%	6688	26

PVSyst	82,28%	98,19%	6,08	1,96	0,104	0,032	47,74%	3509	3205
Sandia	82,33%	98,29%	6,07	1,83	0,103	0,032	64,06%	2413	4301
Akhsassi 2	81,07%	97,57%	6,26	2,38	0,107	0,040	18,68%	5460	1254
Mattei	82,60%	98,67%	6,02	1,43	0,103	0,029	81,35%	1252	5462
Faiman	81,36%	97,93%	6,21	2,22	0,106	0,037	31,87%	4574	2140

To better understand the influence of the data cleaning on the final result we have studied a quality index based on the following facts, if the best model is the one that best describes the minimum variance (maximum R²) and more experimental points (minimum rejection) with a minimum of fluctuations (minimum RMSE), if we attribute to the experimental data a double importance knowing that the more the points are deleted the more the fluctuations are smaller and the more the R² is improved, the models can be classified using the following QA_i quality-Accuracy index: $QA_i = [(1-2*REM)*R^2/RMSE]$ for which the results are shown in Fig. 4. Accuracy-Quality index for the eight stationary models of PV modules thermal behavior.

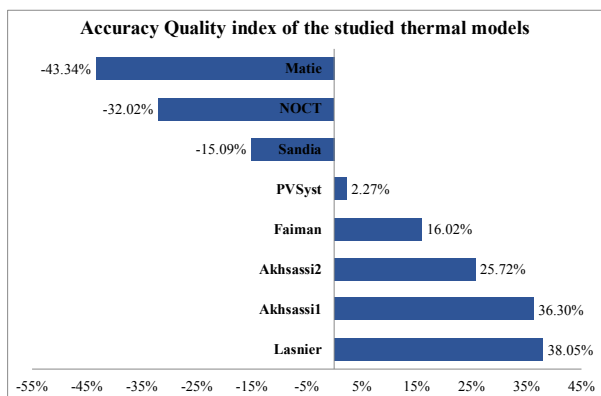


Fig. 4. Accuracy-Quality index for the eight stationary models of PV modules thermal behavior

Mattei, NOCT and Sandia models have all a negative quality index which means that they have deleted at least 50% of the experimental data, as well as PVSyst that eliminates more than 47% of the total points, therefore they are not reliable and cannot be considered as good models for our PV system. In the other hand Faiman and Akhsassi2 have a medium quality index meanwhile Akhsassi1 and Lasnier have reached 36,30% and 38,05%

respectively which makes Lasnier model with the highest quality index the best thermal model among them all.

As mentioned in section 4, to predict the array power of PV system the back-surface, cell temperature is mandatory as one of the inputs used in all the PV DC models, the scope of this part is to calculate PV DC power using the calculated temperature by the different thermal models represented in section 3 instead of the measured module temperature. Thus, 48 models of PV array output were established.

The statistical results of RMSE and R² applied to the relative difference between the calculated and the experimental data are shown in Table 5 and Table 6. Statistical results of correlation coefficient R² between measured and predicted power for the six DC power models using different PV cell temperature models. The lowest RMSE values of 14,82W belongs to Cristofari model and this is coming from the big quantity of deleted points that is varying between 91.08% and 93.34% of removed data. Likewise, the proposed methodology of cleaning excluded many points for Hendrie model with a value ranged between 62.88% and 73.70%. For the results representing Jie, Kroposki, Patel, and Al-Sabounchi models, the cleaning method produced an optimal combination between the values of RMSE and the removed data, except for Kroposki model which excluded 3389 points about 50,48% when used PV cell temperature of Mattei. Generally, the number of eliminated points ranged between 3.10% and 3.75% for Jie model, 3.16% and 50.48% for Kroposki model, 3.26% and 4.87% for Patel model, 2.98% and 4.72% for Al-Sabounchi model. Comparison between Jie, Kroposki, Patel, and Al-Sabounchi models suggests that the best RMSE values after cleaning belongs to the Patel model. Thus, the Patel model configured the best results with the lowest RMSE values and a smaller quantity of data that removed.

Table 5. the root mean squared error (RMSE) before and after cleaning for the six DC power models using different PV cell temperature models

	RMSE Before cleaning (W)						RMSE After cleaning (W)					
	Jie	Kro- poski	Patel	AlSa- bounchi	Hendrie	Cris- tofari	Jie	Kro- poski	Patel	AlSa- bounchi	Hendrie	Cris- tofari
T _{Faiman}	95,63	97,87	94,32	97,39	95,63	94,32	50,69	51,52	48,33	53,54	41,74	15,50
T _{Akhsassi1}	91,46	95,09	90,36	92,91	91,46	90,87	52,34	57,82	50,24	54,87	39,98	15,57
T _{Akhsassi2}	95,87	98,16	94,51	97,67	95,87	94,48	51,1	52,71	48,63	54,02	42,39	15,44
T _{Lasnier}	97,87	100,50	96,26	99,88	97,87	96,00	54,15	58,62	51,47	57,51	38,74	14,82
T _{Mattei}	96,29	96,73	94,45	98,75	96,29	93,65	51,27	19,78	48,19	54,82	40,74	16,36
T _{NOCT}	96,13	97,32	94,54	98,26	96,13	94,09	51,32	30,34	48,49	54,82	39,78	17,83
T _{PVSyst}	95,94	97,89	94,56	97,78	95,94	94,42	50,97	49,43	48,65	54,24	41,38	17,87

T_{Sandia}	95,68	97,40	94,26	97,59	95,68	94,07	50,52	38,05	48,12	53,81	40,78	15,86
--------------	-------	-------	-------	-------	-------	-------	-------	-------	-------	-------	-------	-------

The correlation between measured and predicted PV power depicted in Table 5. the root mean squared error (RMSE) before and after cleaning for the six DC power models using different PV cell temperature models Table 6

and Table 7. Removed data percentage for the six DC power models using different PV cell temperature models indicates a close agreement between the measured and predicted results. The R^2 values are found to be 0.99.

Table 6. Statistical results of correlation coefficient R^2 between measured and predicted power for the six DC power models using different PV cell temperature models

	Jie	Kroposki	Patel	Al-Sabounchi	Hendrie	Cristofari
T_{Faiman}	99,59%	99,54%	99,61%	99,53%	99,40%	97,76%
$T_{Akhassasi1}$	99,54%	99,44%	99,58%	99,50%	99,11%	99,69%
$T_{Akhassasi2}$	99,56%	99,54%	99,60%	99,51%	98,86%	98,39%
$T_{Lasnier}$	99,51%	99,42%	99,56%	99,45%	99,20%	99,72%
T_{Mattei}	99,56%	99,95%	99,61%	99,49%	98,64%	99,70%
T_{NOCT}	99,56%	99,87%	99,61%	99,50%	98,77%	99,62%
T_{PVSyst}	99,56%	99,61%	99,60%	99,51%	98,81%	99,54%
T_{Sandia}	99,57%	99,78%	99,61%	99,51%	98,75%	99,65%

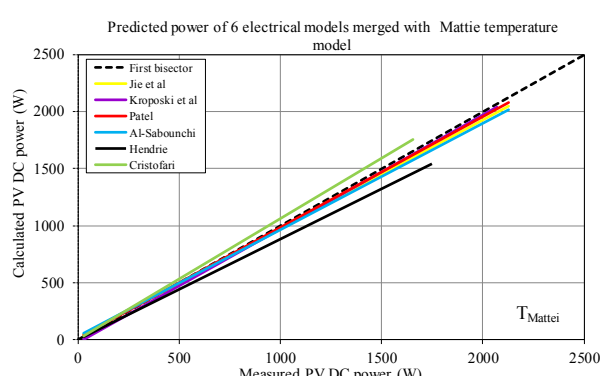
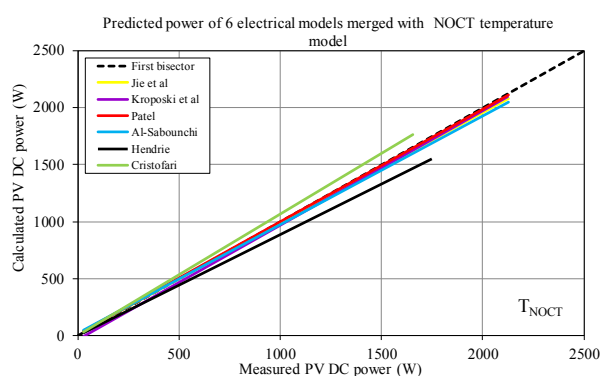
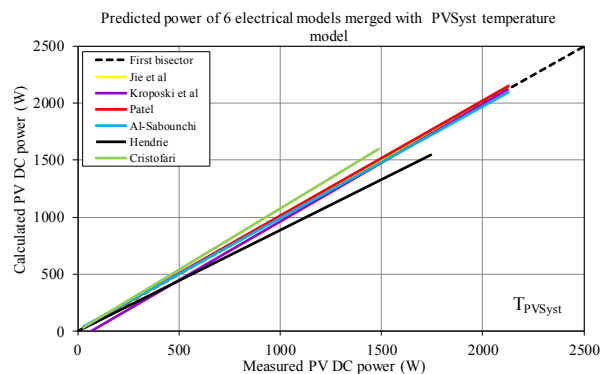
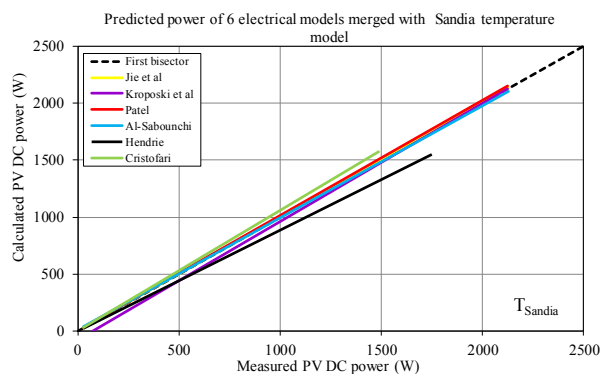
Table 7. Removed data percentage for the six DC power models using different PV cell temperature models

	Jie	Kroposki	Patel	Al-Sabounchi	Hendrie	Cristofari
T_{Faiman}	3,10%	6,00%	3,35%	3,05%	71,79%	92,76%
$T_{Akhassasi1}$	3,44%	3,47%	4,05%	3,22%	71,40%	92,45%
$T_{Akhassasi2}$	3,13%	5,24%	3,40%	3,05%	71,09%	92,79%
$T_{Lasnier}$	3,75%	3,16%3	4,87%	3,20%	70,64%	93,34%
T_{Mattei}	3,75%	50,48%	3,52%	4,72%	73,70%	91,96%
T_{NOCT}	3,23%	28,85%	3,31%	3,29%	62,88%	91,08%
T_{PVSyst}	3,14%	8,10%	3,28%	2,98%	72,36%	91,18%
T_{Sandia}	3,19%	19,48%	3,26%	3,11%	72,98%	92,46%

We can deduce that when Kroposki model is using the temperature of Mattei shows a higher correlation coefficient of 99.95% although it removed 50.48% of the dataset. The best result of the correlation coefficient of the Patel model of 99.61% is achieved when Patel is merged with Faiman, Mattei, NOCT or Sandia temperatures. Likewise, the higher correlation coefficient for Jie is recorded with 99.59% when Jie is merged with the PV cell

temperature of Faiman and having only 3.10% of rejected points. Al-Sabounchi model gives the best results when used with the Faiman's PV cell temperature with a value of 99.53%.

Error! Reference source not found. shows the correlation between predicted PV DC power for each electrical model combined with the eight thermal model



and measured PV DC power.

Hendrie and Cristofari models have always a negative Quality-Accuracy regardless the calculated temperature of

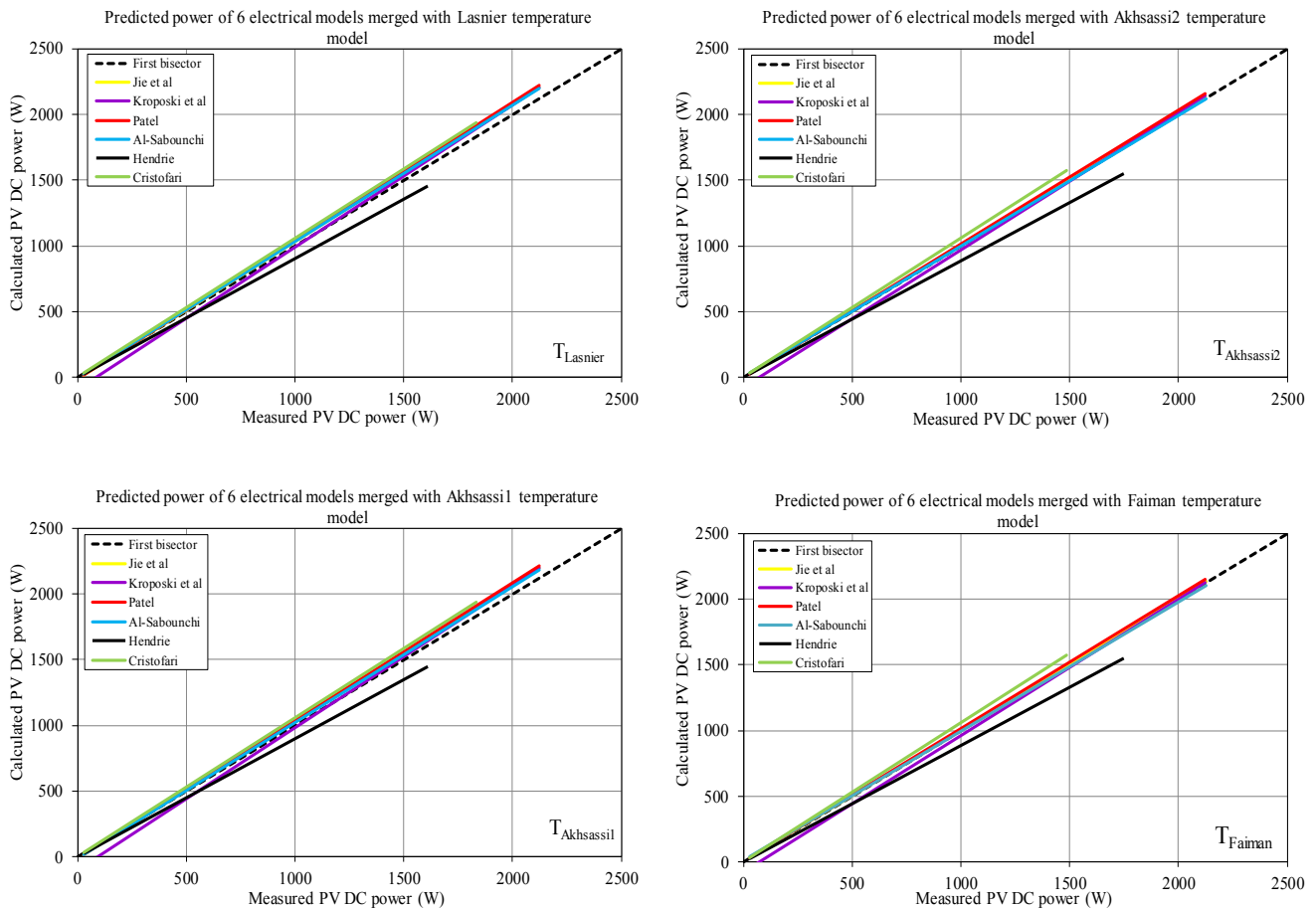


Fig. 5. Correlation between predicted and measured daily PV DC power for six models using different PV cell temperature models

Based on the graphs, it is shown that Hendrie (black line) is under all the other models. The reason why Hendrie model underestimates the PV DC power is because it calculates the PV power using the effective product of transmissivity of glass cover and absorptivity of solar cell $\tau\alpha$ with a value of 0.81. On the other hand Cristofati model (green line) lies below all of the others which implies the overestimation of the PV DC power that can be explained by the positive aggregated value of $\eta_{T_{ref}}AG_T(\gamma \log_{10} G_T)$.

In addition, the Accuracy-Quality index for the 48 electrical models represented in Fig. 6. Quality index for the PV DC power of the 48 electrical studied models, shows that the accuracy of the electrical models does not change no matter which temperature model is used, the order of classification remains the same as following: Patel, Jie, Al-Sabounchi, Kroposki, Hendrie and Cristofari in the last place.

the PV system, thus they are the most unreliable models as they deleted at least half of the total dataset. We can conclude that also the temperature models have an effect on the quantity of removed data for each electrical model knowing that Kroposki electrical model has promptly deleted 50,48% of the total set using Mattei temperature instead of 3.16% using the temperature of Lasnier model.

Patel electrical model gives the highest Accuracy-Quality index and keeps the same place for all the different

5.2. Dynamic regime

temperatures, at the same time Patel model has kept always the best QAI and reached the maximum index using the temperature of Sandia with 1.94% and the minimum index of 1.75% using the temperature of Lasnier Model. Therefor Patel electrical model is concluded as the best accurate model in the present work.

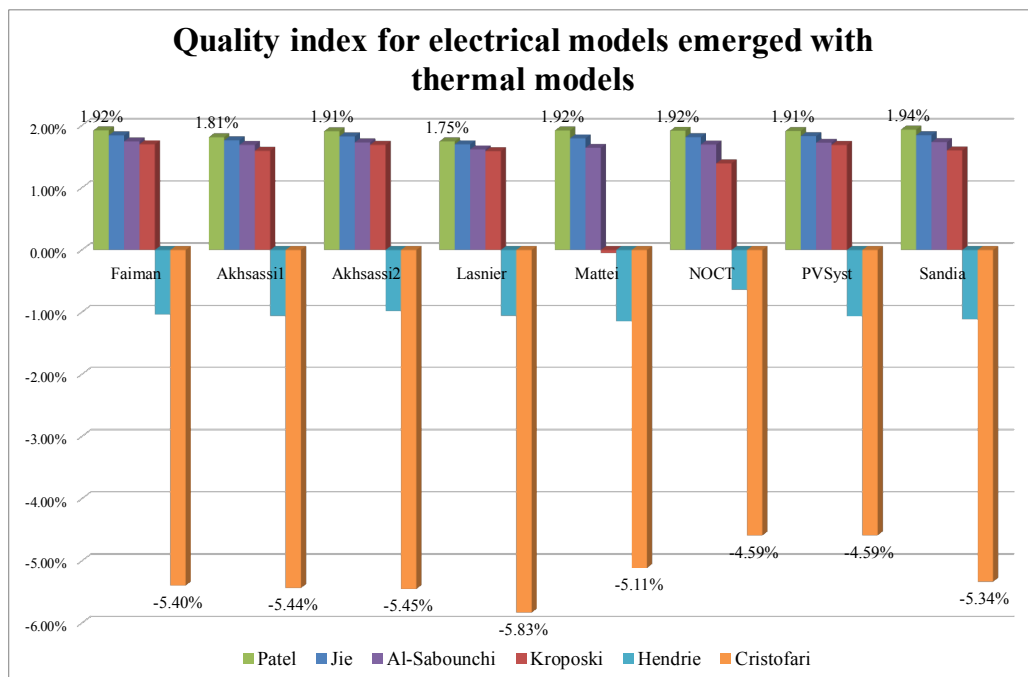


Fig. 6. Quality index for the PV DC power of the 48 electrical studied models

Heat transfer within a PV system only occurs if there are gradients of temperature between the different parts of the system, which implies that the PV system is not at thermodynamic equilibrium (the temperature is not uniform throughout the system). During the transformation of the system to a final state of equilibrium, the temperature will change at the same time with time and space. The purpose of heat transfer analysis is to identify which modes are involved during processing and quantitatively determine how varies the temperature of the system over time. Our dynamic equation of temperature calculation is based on Erraissi findings [21]:

$$\theta_{dyn}(t_{n+1}) = \theta_{dyn}(t_n) + [(\theta_{sta}(t_{n+1}) - \theta_{dyn}(t_n))] * (1 - e^{(-\frac{(t_{n+1}-t_n)}{\tau})}) \quad (16)$$

- $\theta_{dyn}(t_{n+1})$ is the PV temperature at the time t_{n+1} calculated using the equation (16),
- $\theta_{sta}(t_{n+1})$ is the PV temperature at the time t_{n+1} calculated using a stationary model as described in Table 2.
- $\tau = 8mins$

To better concretize the time effect on our study, we compare Lasnier model with the dynamic model for two days separately, the hottest (31 July 2016) and coldest (8 February 2017) days of the studied year. **Error! Reference source not found.**

show the predicted temperatures (Stationary. Left, Dynamic. Right) as function of measured temperature

during the 31st of July 2016 and the 8th of February 2017, respectively.

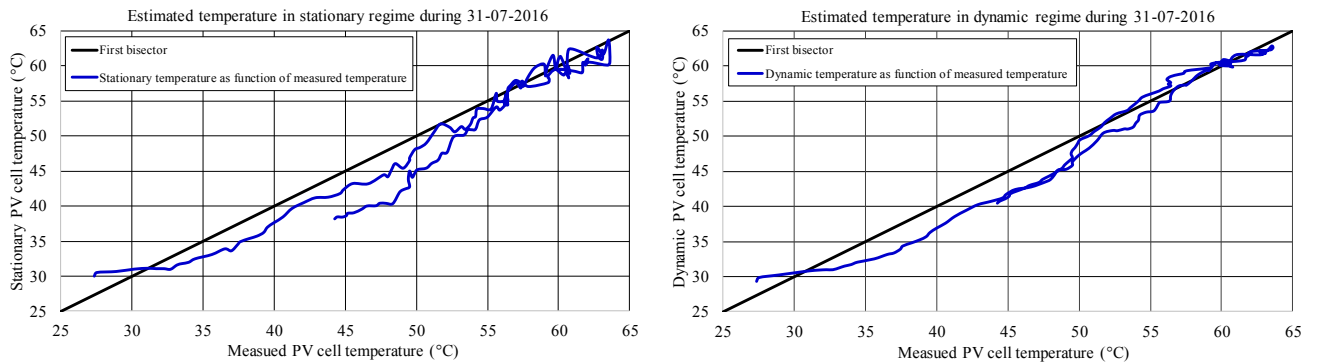


Fig. 7. The predicted (Stationary. Left, Dynamic. Right) versus the measured module temperatures on 31 July 2016

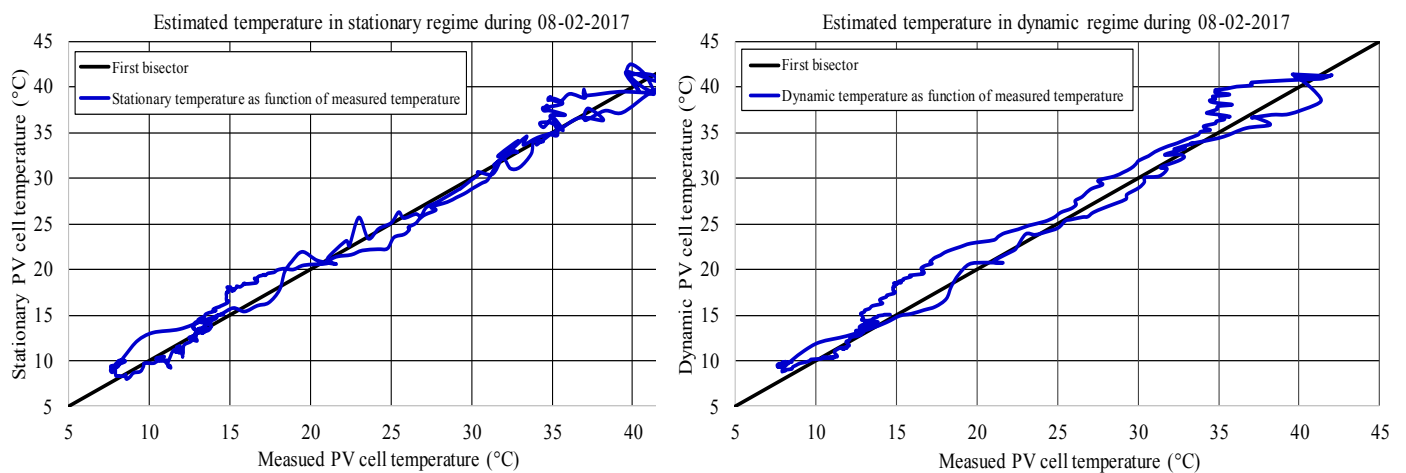


Fig. 8. The predicted (Stationary at left, Dynamic at right) versus the measured module temperatures on 08 February 2017

The illustrations below show that the graph of dynamic temperature is slightly closing comparing to stationary temperature graph in both days which means that the PV temperature is better estimated using dynamic model, also the stationary model has many hysteresis variations unlike the dynamic model that seems more stable and attenuated, this can be simply explained by the fact that in stationary mode, once the radiation is received on the PV module the temperature changes values promptly, while in dynamic mode the temperature takes time to increase or decrease according to the ambient temperature.

To better compare the two models, we have calculated the correlation coefficients projected this time on 1 year of data:

- For dynamic temperature model: $R^2 = 97.19\%$
RMSE= 2.53 °C.
- For stationary temperature model: $R^2 = 97.00\%$
RMSE= 2.61 °C.

Based on all these findings, we can conclude that the dynamic model with higher R^2 and lower RMSE is more reliable than Lasnier model which represents the best stationary model in our study.

Besides, in order adapt Patel electrical model coefficients to our PV cell system we formulate a multilinear equation for the PV power model using solar irradiance and cell temperature. Therefore, the multilinear regression method has been used by defining one function (17) that depends on the total data of solar irradiance, the cell temperature, and that represents the independent variable.

The equation is linear for the unknown parameter (α - β) and is of the form given in Equation (17):

$$\frac{P}{P_{ref}} G_{ref} - G_T = G_T (\alpha - \beta_{ref}) (T_c - T_{ref}) \quad (17)$$

Thus, the dependent function Y can be defined as follows:
 $Y = A.X + Cte$

Where, $Y = \frac{P}{P_{ref}} G_{ref} - G_T$, $X = G_T(T_c - T_{ref})$ and, $A = (\alpha - \beta_{ref})$. The calculated data of stationary temperature and dynamic temperature allowed us to determine the parameter $(\alpha - \beta_{ref})$ as shown in Table 8.

Table 8. Identified parameter

	Calculated with $T_{stationary}$	Calculated with $T_{dynamic}$
$(\alpha - \beta_{ref})$	-0.00463 °C ⁻¹	-0.00444 °C ⁻¹

Error! Reference source not found. shows the predicted versus the measured PV DC power of the two models projected on the 31st of July 2016. Visually no

difference between the graphs can be deduced. Nevertheless, the model using the parameter $(\alpha - \beta_{ref})$ calculated with dynamic temperature gives the best pair of the correlation coefficient and the Root Mean Square Error $\{R^2; RMSE\}$ that is $\{99.55\%; 48.51\text{ W}\}$ against the model using a parameter $(\alpha - \beta_{ref})$ calculated with a stationary temperature that gives $\{99.54\%; 49.25\text{ W}\}$ during one day of study. To compare the two models, we have calculated the correlation coefficients projected this time on 1 year of data using measured PV temperature:

- For dynamic Patel model: $R^2 = 99.53\%$ and $RMSE = 52.89\text{ W}$.
- For stationary Patel model: $R^2 = 99.52\%$ and $RMSE = 53.49\text{ W}$.

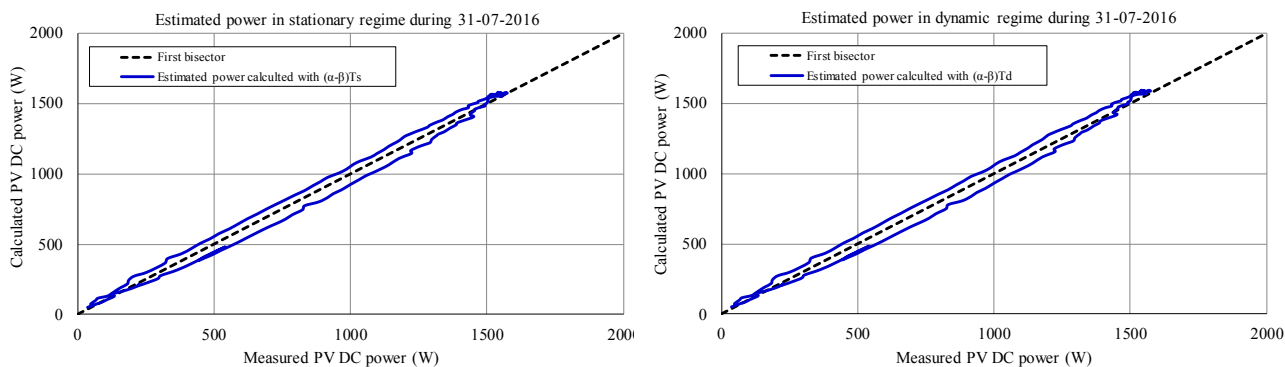


Fig. 9. Predicted (Stationary at left, Dynamic at right) versus the measured PV DC power for 31 July 2016

The same thing is done for both models using different temperatures, measured PV temperature, dynamic temperature, and the best stationary temperature. Fig. 10. The Scatter plots of R^2 and RMSE (W) obtained for the electrical models with $(\alpha - \beta_{ref})$ stationary and $(\alpha - \beta_{ref})$ dynamic for different temperatures ($T_{stationary}$, $T_{dynamic}$, $T_{measured}$) during one studied year. shows the

correlation coefficients during one studied year, for both dynamic and stationary electrical models using different temperatures, the graph shows for all the different temperatures, the dynamic electrical model is always showing the best pair of R^2 and RMSE which means that based on dynamic temperature we can define the best electrical model of a crystalline PV system.

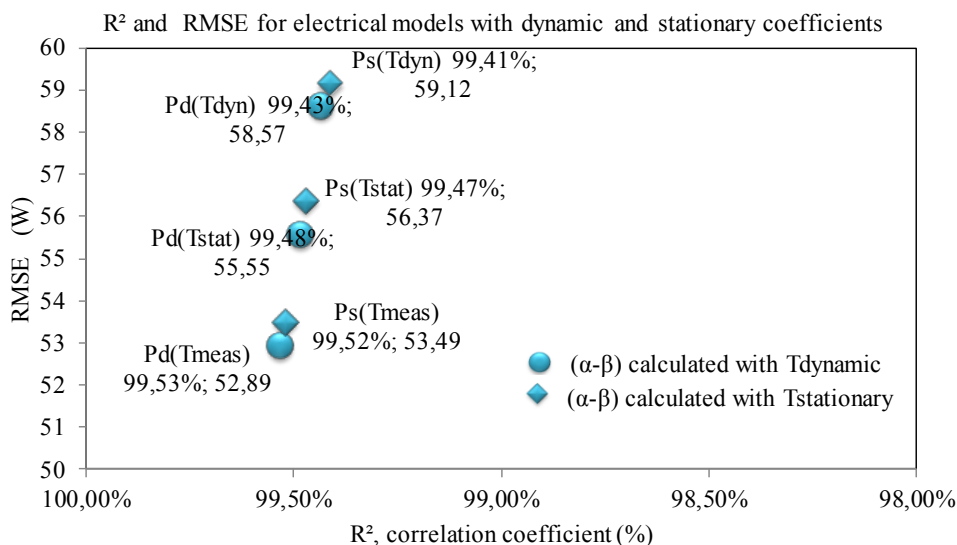


Fig. 10. The Scatter plots of R^2 and RMSE (W) obtained for the electrical models with $(\alpha - \beta_{ref})$ stationary and $(\alpha - \beta_{ref})$ dynamic for different temperatures ($T_{stationary}$, $T_{dynamic}$, $T_{measured}$) during one studied year.

6. Conclusion

In this study, six PV array output models have been used to predict the power produced by a 2 kWp GCPV system installed on the rooftop in the Faculty of Science Semlalia Marrakech. Eight PV module temperature models and one year of measured data were introduced for the PV-module power calculations.

The accuracy of the PV power models was demonstrated by comparing the predictions with the field measured data. Concluding, the results can be summarized as:

- 1- Comparing temperature models with and without wind velocity effect in stationary regime, Lasnier was deduced as the best thermal model among the others as it improved the R^2 and RMSE, by removing less than 0.5% of 6714 data, from 77,44% to 97,16% and from 6,76 °C to 2,53 °C respectively.
- 2- After the amalgamation of the eight thermal models with the six studied electrical models to predict the PV cell power, it was observed that each electrical model reacts differently with each thermal model, best correlation coefficient R^2 for the electrical model of:
 - Kroposki is 99.89% married with Mattei thermal model.
 - Patel is 99.23% calculated with Sandia thermal model.
 - Jie is 99.15% using Sandia thermal model.
 - Al-Sabounchi is 99.04% having Faiman thermal model.
 - Hendrie is 98.4% using Lasnier thermal model.
 - Cristofari 98.36% with Mattei thermal model.

Based on these findings it was found that the Patel model merged with Sandia was the best thermal model even better than Cristofari as Patel's removed only 219 points while Cristofari's removed 3389 from the total of 6714 points.

- 3- Confronting dynamic model with stationary models of the PV cell temperature, the correlation coefficients of R^2 and RMSE were 97.19% 97.00% and 2.53 °C 2.61 °C for the studied dynamic model and Lasnier model respectively. Based on this, it was noted that the dynamic model gives better results than the best of the stationary models.
- 4- The coefficient ($\alpha\text{-}\beta_{\text{ref}}$) used in Patel model was calculated using the dynamic and stationary thermal model to better adapt the electrical model to our PV cell system, after multiple regression it was found that ($\alpha\text{-}\beta_{\text{ref}}$) is equal to:
 - -0.00444 °C-1 using the dynamic thermal model.
 - -0.00463 °C-1 using the stationary thermal model Lasnier.
- 5- After screening the different equations of Patel, it appears that Patel's model with a dynamic coefficient estimates the PV cell power with R^2 and RMSE of

(99.53% and 52.89 W) better than the one with a stationary coefficient (99,52% and 53,49 W).

- 6- In this study, we focused on the effect of solar radiation and cell temperature on the performance of monocrystalline PV system. While it also depends on the incident angle, air mass, dust, inverter efficiency, system technology "Monocrystalline, Polycrystalline or Amorphous" and other system losses. Although it is recommended to focus on the impact of these quantities on the PV performance.

7. Acknowledgement

The equipment used for the work was financed by the Institute for Research in Solar and New Energies IRESEN (Morocco) in the framework of the "Propre.Ma" project from February 2014 to July 2017.

In the name of all the rest of the consortium members, authors would like to thank IRESEN Board and Scientific Committee for financing this through the INNO'PV Program as well as its General Manager, Badr IKKEN, and the management & operations staff for their daily efforts with the 'Propre.Ma' project. Thanks, are also addressed to the Green Energy Park of Benguerir.

References

- [1] E. Kurt and G. Soykan, "Performance Analysis of DC Grid Connected PV System Under Irradiation and Temperature Variations," in *ICRERA 2019, IEEE*, pp. 702–707, 2019.
- [2] I. M. Opedare, T. M. Adekoya, and A. E. Longe, "Optimal Sizing of Hybrid Renewable Energy System for Off-Grid Electrification: A Case Study of University of Ibadan Abdusalam Abubakar Post Graduate Hall of Residence," *Int. J. SMART GRID*, vol. 4, no. 4, pp. 177–189, 2020.
- [3] K. Oda, K. Hakuta, Y. Nozaki, and Y. Ueda, "Characteristics evaluation of various types of PV modules in Japan and U.S.," *IEEE Int. Conf. Renew. Energy Res. Appl. ICRERA 2016*, vol. 5, pp. 977–982, 2016.
- [4] G. Bayrak and M. Cebeci, "Monitoring a grid connected PV power generation system with labview," in *ICRERA 2013, IEEE*, pp. 562–567, 2013.
- [5] A. Belkaid, I. Colak, K. Kayisli, and R. Bayindir, "Improving PV System Performance using High Efficiency Fuzzy Logic Control," *8th Int. Conf. Smart Grid, icSmartGrid 2020*, no. V, pp. 152–156, 2020.
- [6] M. Caruso, R. Miceli, P. Romano, G. Schettino, and F. Viola, "Technical and Economical Performances of Photovoltaic Generation

- Façades,” *Int. J. Smart Grids, ijSmartGrid*, vol. 2, pp. 87–98, 2018.
- [7] T. T. Guingane, D. Bonkougou, E. Korsaga, E. Simonguy, Z. Koalaga, and F. Zougmore, “Modeling and Simulation of a Photovoltaic System Connected to the Electricity Grid with MATLAB/Simulink/Simpower Software,” *8th Int. Conf. Smart Grid, icSmartGrid*, pp. 163–168, 2020.
- [8] E. Skoplaki and J. A. Palyvos, “On the temperature dependence of photovoltaic module electrical performance: A review of efficiency / power correlations,” *Sol. Energy*, vol. 83, no. 5, pp. 614–624, 2009.
- [9] E. Skoplaki, G. Boudouvis, and J. Palyvos, “A simple correlation for the operating temperature of photovoltaic modules of arbitrary mounting,” *Sol. Energy Mater. Sol. Cells*, vol. 92, pp. 1393–1402, 2008.
- [10] S. D. Hendrie, “Evaluation of combined photovoltaic/thermal collectors,” in *Proceedings of ISES Solar World Congress*, no. June, pp. 1865–1869, 1979.
- [11] B. Kroposki, W. Marion, D. King, W. Boyson, and J. Kratochvil, “Comparison of Module Performance Characterization Methods for Energy Production Comparison of Module Performance Characterization Methods for Energy Production,” in *Proceedings of 28th IEEE Photovoltaic Specialists Conference*, no. November, pp. 1407–1411, 2000.
- [12] D. L. King, Kratochvil, J.A., Boyson, W.E., “Temperature coefficients for PV modules and arrays: measurement methods, difficulties, and results”. In: *Proceedings of 26th IEEE Photovoltaic Specialists Conference*, September 29–October 3, Anaheim, CA, 1997.
- [13] M. R. Patel, *Wind and Solar Power Systems*. CRC Press, Boca Raton, FL, §8.6.4, 1999.
- [14] J. Jie, Y. Hua, P. Gang, J. Bin, and H. Wei, “Study of PV-Trombe wall assisted with DC fan,” *Build. Env.*, vol. 42, pp. 3529–3539, 2007.
- [15] C. Cristofari, C. Poggi, P. Notton, and G. Muselli, “Thermal modeling of a photovoltaic module,” in *Proceedings of Sixth IASTED International Conference on “Modeling, Simulation, and Optimization”*, pp. 273–278, 2006.
- [16] A. . Al-Sabounchi, “Effect of ambient temperature on the demanded energy of solar cells at different inclinations,” *Renew. Energy*, vol. 14, pp. 149–155, 1998.
- [17] D. Faiman, “Assessing the Outdoor Operating Temperature of Photovoltaic Modules,” *Prog. Photovoltaics Res. Appl.*, vol. 16, pp. 307–315, 2008.
- [18] M. Mattei, G. Notton, C. Cristofari, M. Muselli, and P. Poggi, “Calculation of the polycrystalline PV module temperature using a simple method of energy balance,” *Renew. Energy*, vol. 31, pp. 553–567, 2006.
- [19] Sandia National Laboratory, An Industry and National Laboratory collaborative to Improve Photovoltaic Performance Modeling, “*Sandia Module Temperature Model*”. (<https://pvpmc.sandia.gov/modeling-steps/2-dc-module-iv/module-temperature/sandia-module-temperature-model/>) (accessed 10 May 2020), 2020.
- [20] N. Aarich, M. Raoufi, A. Bennouna, and N. Erraissi, “Outdoor comparison of rooftop grid-connected photovoltaic technologies in Marrakech (Morocco),” *Energy Build.*, vol. 173, pp. 138-139, 2018.
- [21] N. Erraissi, M. Raoufi, N. Aarich, M. Akhsassi, and A. Bennouna, “Implementation of a low-cost data acquisition system for ‘PROPRE.MA’ project,” *Meas. J. Int. Meas. Confed.*, vol. 117, pp.21-40, 2018.
- [22] M. Akhsassi, A.El Fathi, N.Erraissi, N.Aarich, A.Bennouna, M.Raoufi, A. Outzourhit, “Experimental investigation and modeling of the thermal behavior of a solar PV module,” *Sol. Energy Mater. Sol. Cells*, vol. 180, pp. 271-279 ,2018.
- [23] F. Lasnier and T. Gan Ang, *Photovoltaic engineering handbook*. New York: Adam Hilger, 1990.
- [24] M. Akhsassi, A.El Fathi, N.Erraissi, N.Aarich, A.Bennouna, M.Raoufi, A. Outzourhit, “Confrontation à l’expérience de divers modèles du comportement thermique de modules solaires photovoltaïques,” in *4ème Congr. l’Association Marocaine Therm*, pp. 1–7, 2016.
- [25] Website of PVSyst. (<http://www.pvsyst.com/en/>) (accessed 10 May 2020), 2020.
- [26] P. Nalay, “Développement d’une Méthode Générale d’analyse des Systèmes Photovoltaïques,” 1987.
- [27] D. L. King, J. Kratochvil, and W. Boyson, “Photovoltaic array performance model,” vol. 8, pp. 1–19, 2004. Report SAND2004-3535.
- [28] Sandia National Laboratory, An Industry and

National Laboratory collaborative to Improve Photovoltaic Performance Modeling, "*PV_{syst} Cell Temperature Model*".
(<https://pvpmc.sandia.gov/modeling-steps/2-dc-module-iv/cell-temperature/pvsyst-cell-temperature-model/>) (accessed 10 May 2020),

2020.

- [29] M. Koehl, M. Heck, S. Wiesmeier, and J. Wirth, "Modeling of the nominal operating cell temperature based on outdoor weathering," *Sol. Energy Mater. Sol. Cells*, vol. 95, pp. 1638–1646, 2011.